Structure and Ionic Conductivity of a Series of Di-*o*-butyrylchitosan Membranes

Ying Wan, Katherine A. M. Creber, Brant Peppley, V. Tam Bui

Department of Chemistry and Chemical Engineering, Royal Military College of Canada, P.O. Box 17000, Station Forces, Kingston, Ontario, Canada, K1K 7B4

Received 2 March 2004; accepted 10 July 2004
DOI 10.1002/app.21175
Published online 22 October 2004 in Wiley InterScience (www.interscience.wiley.com).

ABSTRACT: Di-*o*-butyrylchitosan was prepared by reacting chitosan with butyric acid anhydride in the presence of perchloric acid as a catalyst. ^{13}C-NMR and IR spectra of the modified chitosan suggested that both hydroxyl groups, at the C-6 and C-3 positions, in the chitosan molecules were substituted. The maximum degree of substitution was found to be less than 28%. The results of X-ray diffractograms revealed that, in comparison with the unmodified chitosan membrane, the crystallinity of di-*o*-butyrylchitosan membranes was remarkably decreased. Meanwhile, it was also observed that the swelling indices of modified membranes were increased significantly in direct proportion to the degree of substitution. Thermogravimetric analysis indicated that the modified membranes exhibited a slightly increased thermal stability compared to the unmodified membrane. The ionic conductivity of di-*o*-butyrylchitosan membranes after hydration was investigated using impedance spectroscopy. Compared to the unmodified chitosan membrane, the hydrated di-*o*-butyrylchitosan membrane with a relatively high degree of the substitution showed an increased ionic conductivity of more than one order of magnitude. © 2004 Wiley Periodicals, Inc. J Appl Polym Sci 94: 2309–2323, 2004

Key words: modified chitosan membrane; hydration; ionic conductivity; fuel cell

INTRODUCTION

Many kinds of polysaccharides are produced in large quantities in nature. Of these naturally occurring polymers, chitin is the second most abundant, with cellulose being first. Chitin is obtained mainly in lower animals such as shrimp, crab, lobster, squid, and even beetles, and it may also be found in certain fungi and yeast.[1] Chitin has a molecular structure that is similar to cellulose, but it is an amino polysaccharide having acetamide groups at the C-2 positions in place of hydroxyl groups at the same positions in cellulose. Chitosan, a principle derivative of chitin, can be obtained by deacetylating chitin. In addition, chitosan itself also occurs in nature in some fungi, and it can be isolated from cell walls of these fungi.[2] The chemical structures of chitin and chitosan are illustrated in Figure 1.[3]

A great deal of interest has been aroused in chitosans as special polymeric materials because of their specific properties such as biodegradability, biocompatibility, and bioactivity. Chitosan also has a high potential for developing sophisticated functional polymers quite different from those of synthetic polymers since it has both free amino groups and hydroxyl groups on its backbone, which are easily modified by some organic reactions.[4] Chitosan can be readily converted to fibers, films, coatings, and beads, as well as powders and solutions, and it has been widely used in many areas such as pharmaceutical and biomedical engineering, paper production, textile finishes, photographic products, cements, heavy metal chelation, waste water treatment, and fiber and film formation for at least the last two decades.[5]

Due to the presence of amino groups, chitosan is a cationic polyelectrolyte.[6] Chitosan membrane has been used for active conduction of chloride-ion in aqueous solution,[7] which can also be represented as ion-conducting. A chitosan membrane has a very low electrical conductivity in its natural state (dry state). However, in its wet state (swollen in water), its amino groups can be partially protonated and thus may contribute to ionic conduction in the membrane. Owing to a strong micellular structure through intramolecular and/or intermolecular hydrogen bonding, chitosan membrane has poor swelling capacity in water,[8,9] which obviously hinders the ionic transport in the membranes. Many efforts are being directed toward disrupting the rigid crystalline structure of chitosan and the development of soluble chitosan derivatives using acylation[10–12] or alkylation[13,14] reactions with longer or more bulky groups, even though the degree

Correspondence to: K. A. M. Creber (creber@rmc.ca).
Contract grant sponsor: National Science and Engineering Council of Canada; contract grant number: 239090–01.

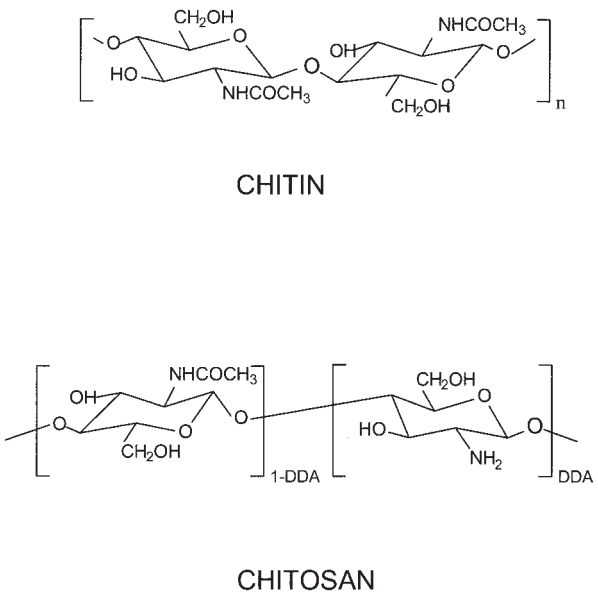

Figure 1 Chemical structure of chitin and chitosan (DDA is the degree of deacetylation).

of substitution is relatively low in many cases. However, some chemical modifications, introducing acyl groups or alkyl groups to the C-6 or C-3 positions, were found to enhance the solubility properties, mainly in organic solvents and not in water in most cases.

The results from our previous work reveal that the chitosan membrane made from unmodified chitosan with high molecular weight and an appropriate degree of deacetylation shows an ionic conductivity around 10^{-4} S.cm^{-1} after hydration for 1 h at 25°C. This is still relatively low for practical applications.[15] The low ionic conductivity of chitosan membrane may mainly be attributed to its crystalline region, which hinders the ion migration. One effective method to reduce the crystalline part of chitosan membrane is to crosslink the membrane with appropriate crosslinking agents, for example, glutaraldehyde (GA). GA can react with amino groups in chitosan units to form a Shiff's base, leading to a reduction in the amino group concentration that is responsible for the ionic conductivity of the membrane. In addition, a too high crosslinking density might also decrease the swelling index of crosslinked membrane, which is related to the ionic conductive performance of the membrane. It is obvious that the beneficial effect of the crosslinking density on the ionic conductivity of the chitosan membrane must outweigh the unfavorable effects resulting from the reduction of the amino groups and the swelling index of crosslinked membranes. Indeed, by a careful optimization of the crosslinking density, an increase in the ionic conductivity of hydrated chitosan membranes of around one order of magnitude has been achieved.[16]

Chemical modification may provide other useful ways to improve the ionic conductivity of chitosan membrane. However, it is worth mentioning that, for the present application, chemical modification should be conducted at the C-6 or C-3 position in chitosan units to maintain the amino group function at the C-2 position unchanged, which is mainly responsible for the ionic conductance. For improvement of the ionic conductivity of chitosan membrane, a phosphorylated chitosan membrane with appropriate phosphorus content had been previously investigated but its ionic conductivity, after hydration, shows only a slight increase because of the crosslinking effect from the condensation of phosphates when the phosphorus content is higher.[17] In the present study, a modified chitosan membrane was achieved by reacting chitosan with butyric acid anhydride in the presence of perchloric acid as a catalyst. It is expected that some hydroxyl groups on the chitosan units will be replaced by the larger and more bulky butyryl groups, which should partially destroy the crystalline structure in the chitosan membrane; thus, the hydrophilicity and the swelling property of the modified membrane should consequently be improved, which could help ions migrate through the membrane more easily and provide the modified membrane with an improved ionic conductivity.

EXPERIMENTAL

Materials and reagents

Chitosan (shrimp-based product) was received in the form of flake with a claimed high molecular weight from Sigma-Aldrich Canada Ltd. (Oakville, Canada). All other chemicals were obtained and used as reagent grade from either Sigma-Aldrich Canada Ltd. or Caledon Laboratories Ltd. (Georgetown, Canada): acetic acid (99.7%), sodium acetate (99%), *N*-acetyl-D-glucosamine (99%), sodium hydroxide pellets, butyric acid anhydride (99%), perchloric acid (71%), diethyl ether (99%), deuterium oxide (99.9 atom % D), ammonium hydroxide (38%), and methanol (99%). Sodium 3-(trimethylsily) propionate-2,2,3,3-d_4 (TSP, 98 atom % D) and acetic acid-d_4 (99.6 atom % D) were provided by CDN ISOTOPES INC. (Montreal, Canada). Deionized water (resistivity $> 1.8 \times 10^8$ Ωcm) was used for all samples.

Degree of deacetylation and molecular weight of chitosan

The original chitosan sample was treated in 50 wt % NaOH aqueous solution under air for 1 h, at 100°C to increase its degree of deacetylation. The reaction product was washed subsequently in deionized water until a neutral pH was reached, and then dried in a con-

vection oven at 50°C for 2 days. The process was repeated one more time using the sample from the reaction product of the first deacetylation step with the same reaction conditions under air for 2 h, at 100°C. This product was also washed repeatedly in deionized water until reaching a neutral pH. The samples were dried first in a convection oven at 50°C for 2 days and then in a vacuum oven at 50°C for 24 h.

First derivative UV spectra were recorded on a CARY 5E UV-VIS-NIR spectrometer,[18] and used for calculating the degree of deacetylation (DDA) of chitosan. A calibration curve from *N*-acetyl-D-glucosamine was generated according to our previously reported method.[19] The water content of chitosan samples was determined using TGA (Thermogravimetric Analysis) and it was considered as the largest contributing factor to the error in the DDA calculation.

The viscosity-average molecular weight of chitosan was examined using 0.25*M* CH_3COOH/0.25*M* CH_3COONa as solvent system.[20]

Preparation of di-*o*-butyrylchitosan membranes

Di-*o*-butyrylchitosan was prepared following a reported method.[21] Powdered chitosan (5g) was added into a 250 mL flask containing a freshly prepared mixture of butyric acid anhydride (50 mL) and perchloric acid (2.5 mL). The mixture was stirred for variable time between 1 ~ 3 h to obtain the different degrees of substitution while the temperature was maintained within a 20 ~ 30°C range by means of a water-cooling bath as this reaction was an exothermic one. The reaction product obtained by filtration was washed first with ether three times and then with deionized water five times. The solid product was suspended in water, neutralized to pH 7 with ammonium hydroxide solution, and boiled for 10 min to remove any traces of acid. The derivatives formed were washed thoroughly with water, and were dried in a convection oven at 50°C for 2 days.

The dried di-*o*-butyrylchitosans were dissolved in 1% (by volume) aqueous acetic acid with a ~ 1.5 wt % di-*o*-butyrylchitosan concentration. These solutions were filtered and cast into membranes. After drying in air, the di-*o*-butyrylchitosan membranes were neutralized using a mixture of ammonium hydroxide and methanol (1 : 8 by volume) for about 1 h. Finally, the membranes were washed intensively with deionized water until reaching a neutral pH, and were dried again at 25°C. All modified membranes in the dry state had almost the same average thickness of 0.2 (±0.013) mm.

FTIR spectra

The infrared spectra of the membranes were recorded on a Nicolet 510P Forrier-Transform-IR (FTIR) spectrometer with a resolution of 2 cm^{-1}, 128 scans, in transmission mode, and the sample chamber was purged with dry nitrogen gas. The membranes were dried to a constant weight before spectra were recorded. The average thickness of the membranes was around 30 μm.

NMR spectra

^{1}H-NMR measurements were performed on a Bruker Avance-500 (dmx-500) NMR spectrometer at room temperature. A ~ 5 mg powdered sample was dried in a vacuum oven at 50°C for 2 days, and then was introduced into a 5mmϕ NMR tube. The sample was further vacuum dried at 50°C for 2 days, after which 0.5 mL of 2 wt % CD_3COOD/D_2O solution was added. The tube was kept at 70°C to dissolve the polymer in solution for 24 h. ^{1}H-NMR chemical shifts were expressed in ppm downfield from the signal for sodium 3-(trimethylsily)propionate (TSP) as an external reference.[22]

^{13}C-NMR measurements were carried out on the same NMR spectrometer but the temperature was kept at 70°C. A 300 mg powdered sample (separated by a 100 mesh sieve) was placed into a 10 mL picnometer, and dried in a vacuum oven at 50°C for 2 days. To this sample, 6 mL of 2 wt % CD_3COOD/D_2O solution was introduced, and the mixture was allowed to dissolve at 70°C for 24 h with stirring. Subsequently, the mixture was cooled to 40°C, to which 50 μL of 0.5*M* KNO_2/D_2O was added with vigorous stirring for 20 min, and then was rapidly cooled to room temperature or lower. The solution was filtered, and a ~ 1.0 mL of this solution was introduced into a 5 mmϕ NMR test tube for ^{13}C-NMR measurement.

Thermal analysis

Thermogravimetric graphs (TGA, Texas Instruments 2050) were used to investigate the thermal stability of the modified chitosan membranes. Each membrane sample (5–10 mg) was run from 25 to 400°C at a scanning rate of 10°C/min under a nitrogen atmosphere. The onset temperature of thermal degradation was examined for the analysis of the thermal stability.

Wide-angle X-ray diffractometry

A SCINTAG X1 X-ray diffractometer was used to record the wide-angle X-ray diffractograms of membranes at 25°C. The X-ray source was Ni-filtered Cu-Kα radiation (45 kV and 40 mA). The dried membranes were mounted on aluminum frames and scanned from 5 to 45° (2θ) at a speed of 2°/min. To measure percent relative crystallinity of the membranes, the amorphous areas and the area of crystalline peaks were measured and the percent relative

TABLE I
Degree of Deacetylation and Viscosity-Average Molecular Weight

Sample code	DDA (%)	water + impurities (%)	M_v
ChT	77.3 (±2.1)	4.1 (±0.3)	2.17 (±0.13) × 10^6
ChT2	97.4 (±2.3)	2.9 (±0.1)	4.75 (±0.21) × 10^5

crystallinities (X_c) were calculated via the following formula[23]:

$$X_c = [A_c/(A_c + A_a)] \times 100\% \quad (1)$$

where A_c and A_a are the areas of crystalline and amorphous regions, respectively. Three measurements were made for each sample.

Swelling index

The dry membrane (mass = W_d) was immersed in an excess amount of deionized water at 25°C until swelling equilibrium was obtained (normally, around 1 h at ambient temperature). The mass of the wet membrane (W_w) was attained after gently removing the surface water with blotting paper. Five specimens were measured for each sample. Swelling index (SI) was then calculated on the basis of the masses of wet membrane and dry membrane via the formula:

$$SI = [(W_w - W_d)/W_d] \times 100\% \quad (2)$$

Ionic conductivity

The conductance measurements were carried out by following a reported method.[24] A Hewlett-Packard Impedance/Gain-Phase Analyzer (model 4194A) was used for the impedance spectroscopic analysis of the membranes. Complex impedance measurements were made in the AC mode (0.1–10^4 kHz) and 1 V amplitude of the applied signal. The dry membranes were sandwiched between two brass blocking electrodes in the measurement cell. For the impedance analysis in the swollen state, the membranes were immersed in deionized water at room temperature for the required time. Before starting measurements, the surface water was gently removed, and the swollen membrane was placed quickly between two electrodes in the measurement cell. The water content of the membrane was assumed to remain constant during the short period of time required for making the measurement. Five measurements were made for each sample.

RESULTS AND DISCUSSION

Chitosan and modified chitosan

Since the higher content of amino groups in chitosan membranes may contribute to a higher ionic conductivity, the chitosan samples were deacetylated before the preparation of the membranes. The original chitosan sample and deacetylated chitosan sample are code-named as ChT and ChT2, respectively. The degree of deacetylation and viscosity-average molecular weight obtained for the original and deacetylated chitosan samples are listed in Table I. Although it is somewhat difficult to completely deacetylate chitosan, a high DDA value can be reached if successive treatments are employed.[25] As shown in Table I, the DDA of ChT2 reached a value as high as 97.1% by being successively deacetylated twice, and it had not been substantially degraded compared to the original chitosan sample (ChT) as shown by only a slight decrease in molecular weight. The 0.25*M* CH_3COOH/0.25*M* CH_3COONa solvent system was chosen to determine the viscosity-average molecular weight of chitosan because this solvent system is almost independent of its DDA in a range above 70%. With this solvent system, the viscosity-average molecular weight of chitosan is determined using the following equation[20]:

$$[\eta] = 1.40 \times 10^{-4} M_v^{0.83} \quad (3)$$

where η and M_v are the intrinsic viscosity and the viscosity-average molecular weight, respectively.

In addition, ChT and ChT2 were reacted with butyric acid anhydride under the same conditions with various reaction times. Two series of di-*o*-butyrylchitosan, and corresponding membranes, were obtained. They were designated as ChT-B30, ChT-B60, ChT-B90, ChT-B120, ChT-B150, and ChT2-B60, ChT2-B90, ChT2-B120, ChT2-B150, ChT2-B180, respectively, where B refers to butyrylation reaction, and the number following the B indicates the reaction time in minutes.

Infrared analysis

Infrared spectra of the unmodified membranes and two modified chitosan membranes are shown in Figures 2 and 3, respectively. The IR spectrum of ChT sample in Figure 2 shows a broad strong band around 3400 cm^{-1} for OH and NH stretch, two weak CH stretch bands at 2920 and 2867 cm^{-1}, an amide I band at 1655 cm^{-1}, and an amide II band at 1585 cm^{-1}. The bands at 1153, 1071, and 1029 cm^{-1} can be assigned to the saccharide structure, and some other bands at 1415, 1374, and 1318 and 1255 cm^{-1} may be related to the bending bands of OH and CH. In the case of the

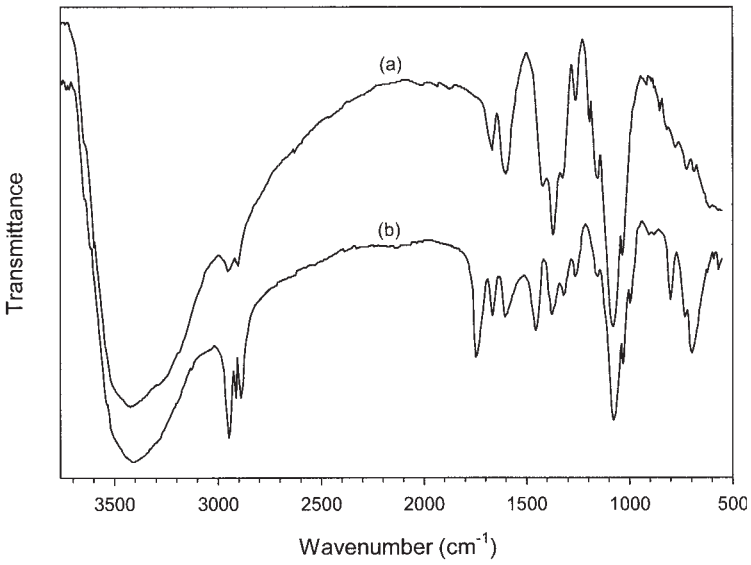

Figure 2 Infrared spectra of chitosan and modified chitosan: (a) ChT, and (b) ChT-B120.

ChT2 sample, in Figure 3, the OH stretching band is slightly shifted to a higher wavenumber (around 3500 cm^{-1}) with a weak shoulder near 3360 cm^{-1}. The amide I band, at 1655 cm^{-1}, nearly disappears and only a small shoulder is observed. All other bands are found at substantially the same wavenumbers, changing only in intensity. These results are consistent with published reports.[26]

In comparison with the infrared spectrum of ChT, the characteristic absorptions of the amine groups at 1655 cm^{-1} and 1585 cm^{-1} can still be observed, for ChT-B120 in Figure 2, but a few new bands have appeared. There are two new strong bands, at $\sim$ 1735 cm^{-1} and $\sim$ 1457 cm^{-1}, which can be assigned to carbonyl groups.[27,28] The other new absorption bands, near 2970, 2860, 785, and 743 cm^{-1}, may be assigned to the rocking mode of aliphatic $-CH_2-$ and $-CH_3$ of the butyryl group.[21,29] When compared to the ChT-B120, ChT2-B150 shows a similar IR spectrum except that the amide I band of ChT-B120, at 1655 cm^{-1} in Figure 2, is replaced by a shoulder in Figure 3. Meanwhile, it is also noted that, for ChT-B120 (Fig. 2) and ChT2-B150 (Fig. 3), both intensities of absorption, due to primary hydroxyl groups at around 1030 cm^{-1}, and due to secondary hydroxyl groups near 1070 cm^{-1}, have become smaller than that of corresponding ChT and ChT2, which can be found out using the integration

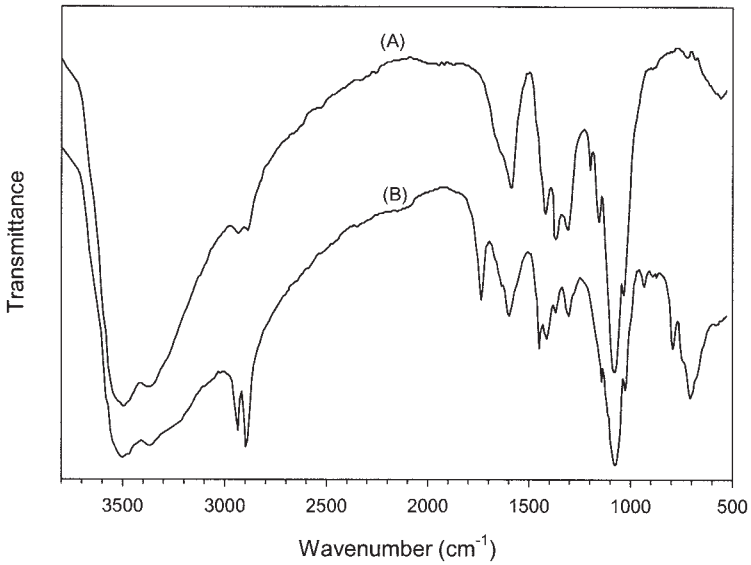

Figure 3 Infrared spectra of chitosan and modified chitosan: (A) ChT2, and (B) ChT2-B150.

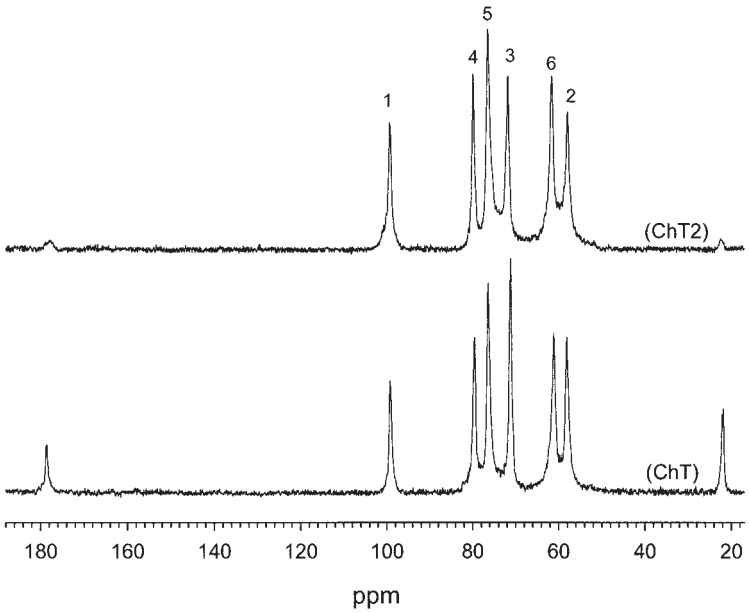

Figure 4 ^{13}C-NMR spectra of chitosan.

of peak areas. These results suggest that: (1) some hydroxyl groups in ChT-B120 or ChT2-B150 have been substituted by the butyryl groups, and (2) the substitution in ChT-B120 and ChT2-B150 probably occurred both at the C-6 and the C-3 positions on the chitosan units.

^{13}C and ^{1}H-NMR spectra

^{13}C-NMR measurements were made to further examine the positions of substitution on the chitosan units. ^{13}C-NMR spectra of ChT and ChT2 are shown in Figure 4. There is little difference between their NMR spectra except for the peak strength at ~ 22 and ~ 179 ppm, which is associated with the acetamide methyl groups and acetamide carbonyl groups, respectively. This can be easily understood since ChT and ChT2 have almost the same chemical structure but different contents of amino groups.[30,31] The ^{13}C-NMR spectra of ChT-B120 and ChT2-B150 are represented in Figures 5 and 6, respectively. It is observed again that the spectrum of ChT2-B150 is almost the same as that of ChT-

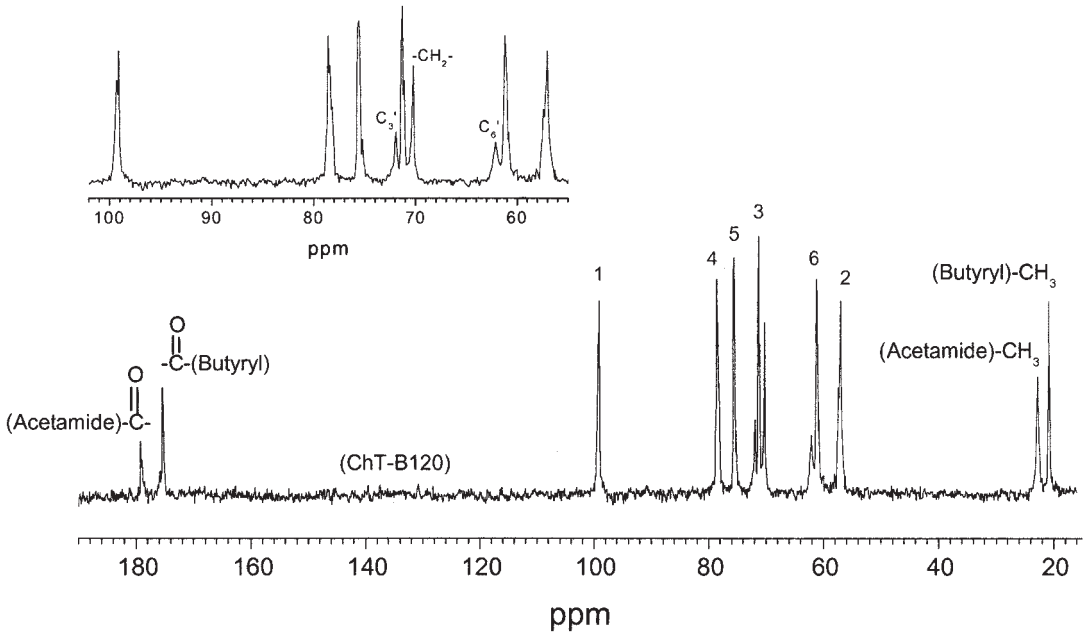

Figure 5 ^{13}C-NMR spectra of di-*o*-butyrylchitosan (ChT-B120).

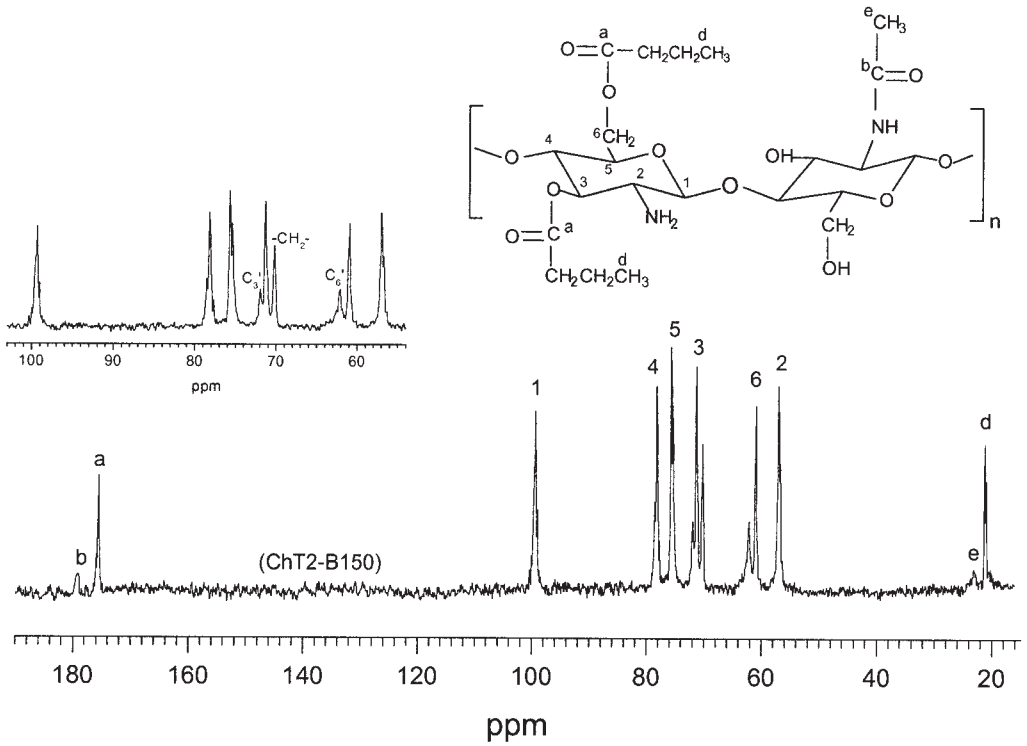

Figure 6 ^{13}C-NMR spectra of di-*o*-butyrylchitosan (ChT2-B150).

B120 except for the change in intensity for two peaks at ~ 22 and ~ 179 ppm. Compared with Figure 4, the characteristic series of peaks of chitosan are still retained; a few new peaks appear near 20.1, 61.9, 70.2, 71.8, and 174.9 ppm in Figure 5 or Figure 6 for ChT-B120 or for ChT2-B150. The signal at 61.9 ppm may be assigned to the substituted C-6, which is indicated by C_6 ′ in Figure 5, according to the ^{13}C-NMR studies for glucose and the solid chitin.[32] Since the signal of the carbon attached to the glucose could be slightly shifted to a lower magnetic field when blocked with a methyl group,[33] it may suggest that the signals at ~ 71.8 ppm correspond to the substituted carbon at the C-3 position of the chitosan unit, which is indicated by C_3 ′ in Figure 5. According to Tokura's result for ethyl-chitin,[34] it is reasonable that the signals at around 70.2 ppm should be assigned to the methylene of the butyryl groups. The signals at ~ 20.1 ppm and ~ 174.9 ppm can be related to the methyl groups and carbonyl groups of the butyryl groups, respectively, based on Cha's report for chitooligosaccharide.[35] These results, therefore, suggest that both hydroxyl

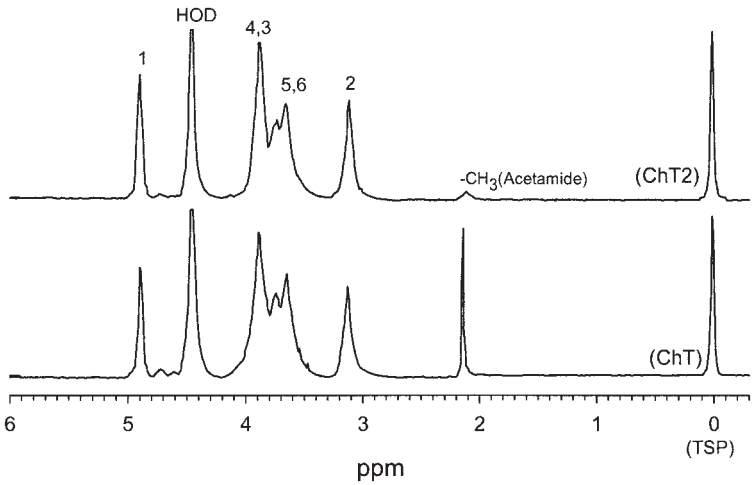

Figure 7 ^{1}H-NMR spectra of chitosan.

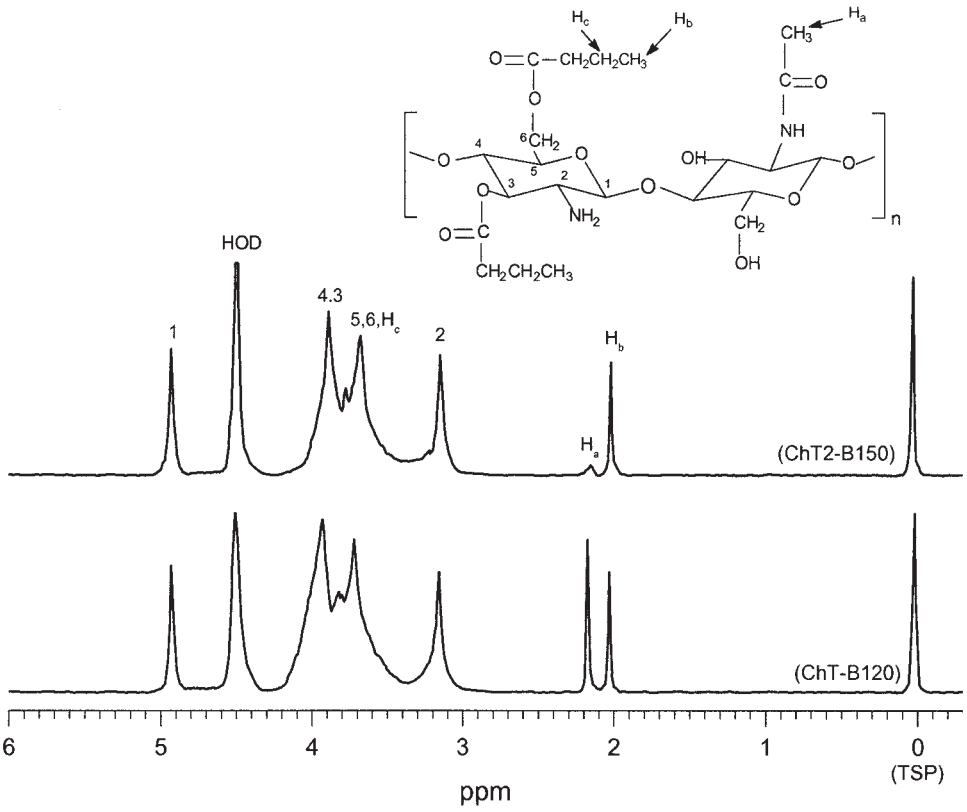

Figure 8 ^{1}H-NMR spectra of di-*o*-butyrylchitosan.

groups at the C-6 and the C-3 positions are substituted for the ChT-B120 and the ChT2-B150.

Based on the above assignments, the ^{1}H-NMR spectra of modified chitosan were used to estimate the degree of substitution by comparison of the peak areas between the di-*o*-butyrylchitosan and unmodified chitosan. The ^{1}H-NMR spectra of ChT and ChT2 are represented in Figure 7, which is in agreement with published reports of chitosan,[22] and the ^{1}H-NMR spectra of ChT-B120 and ChT2-E150 are illustrated in Figure 8. Peaks corresponding to the methyl groups on the butyryl groups and acetamide groups were integrated and compared; the degree of substitution for C-6 or C-3 has not been further distinguished because the proton peaks of the methyl group on the butyryl group are superimposed in their ^{1}H-NMR spectra regardless of whether they are attached to C-6 or C-3 position. The degree of substitution, for all samples, is listed in Table II. It is observed that the degree of substitution gradually increases with the reaction time, and the highest degree of substitution is less than 28%, which means that approximately one of every four chitosan units has been substituted. In fact, the degree of substitution could not be increased further under current reaction conditions even when the reaction time was increased further. In addition, it was also found that the degree of substitution is significantly lower for one set of samples with higher DDA. For example, the degree of substitution of ChT-B120 is higher than that of ChT2-B120. A possible explanation

TABLE II
The Degree of Substitution (DS) of Modified Chitosan[a]

Sample code	Degree of substitution (%)	Sample code	Degree of substitution (%)
ChT-B30	11.3 (±1.3)	ChT2-B60	14.4 (±0.9)
ChT-B60	18.6 (±1.1)	ChT2-B90	18.5 (±1.0)
ChT-B90	21.2 (±1.2)	ChT2-B120	21.7 (±1.1)
ChT-B120	24.4 (±1.4)	ChT2-B150	23.3 (±1.2)
ChT-B150	27.2 (±1.2)	ChT2-B180	25.9 (±1.1)

[a] The DS percentage values were determined from the peak at ~ 2.03 ppm (methyl protons of the butyryl groups) and the peak at ~ 2.15 ppm (methyl protons of the acetamide), as seen in Fig. 8.

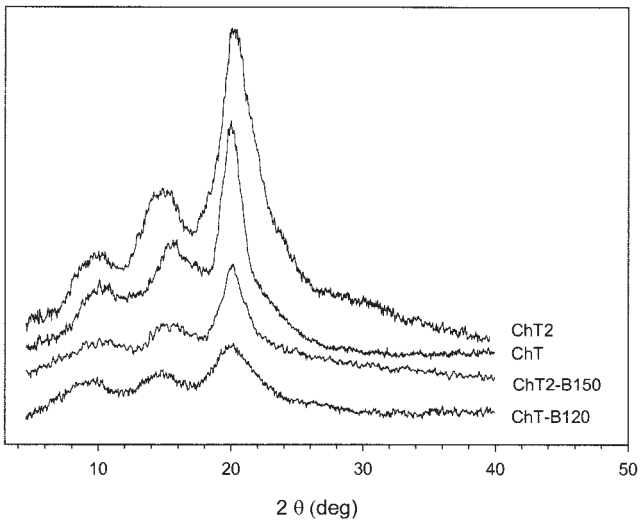

Figure 9 X-ray diffraction patterns of chitosan and di-*o*-butyrylchitosan membranes.

for the difference between these two sets of samples may arise from their DDA values. Chen's results suggest that chitosan with higher DDA is more flexible, and more flexible chains of chitosan will facilitate the hydrogen-bonding formation and, in turn, a higher degree of crystalline formation[36]; as a result, the reactant is prevented from entering the micelle (especially for those micelles in the crystalline region) for the following modification reactions, leading to a lower degree of substitution for modified chitosan that has a higher DDA value.

Crystallinity and swelling index of di-*o*-butyrylchitosan chitosan membranes

The X-ray patterns of unmodified and modified chitosan membranes are illustrated in Figure 9, and the corresponding crystallinity and swelling index are represented in Figures 10 and 11, respectively. The diffractogram of the membranes in Figure 9 consists of three major crystalline peaks locating around 10°(2θ), 15°(2θ), and 20°(2θ), which are in agreement with Samuels's report.[37] The X-ray patterns indicate that, compared to unmodified chitosan membrane, the crystalline structure of di-*o*-butyrylchitosan membranes has not been obviously modified but the peak intensity has decreased markedly. It is also noted that, in Figures 10 and 11, the crystallinity of di-*o*-butyrylchitosan membrane decreases remarkably with increasing degree of substitution. It is well known that the rigid crystalline structure of chitosan is mainly stabilized by the hydrogen bonding. The intramolecular hydrogen bond is mainly formed by an amino group at C-2 and a hydroxyl group at C-3 positions. The intermolecular hydrogen bond can be formed between hydroxyl groups at C-6 and C-3 through an absorbed water molecule. Part of intermolecular and intramolecular hydrogen bonds in chitosan will be reduced after the butyryl groups are incorporated because these substituted groups are much longer and bulkier than those original hydroxyl groups at the C-6 or C-3 positions, and give a greater degree of steric hindrance to formation of new hydrogen bonds. As a result, modified membranes are expected to show decreased crystallinity.

As can be seen in Figures 10 and 11, the swelling index of di-*o*-butyrylchitosan membranes increases with increasing degree of substitution and then slightly decreases. In general, it is known that the swelling properties of chitosan membranes are simultaneously controlled by both the crystallinity and the hydrophillicity of groups on the chitosan units. Normally the growing crystalline portion in the mem-

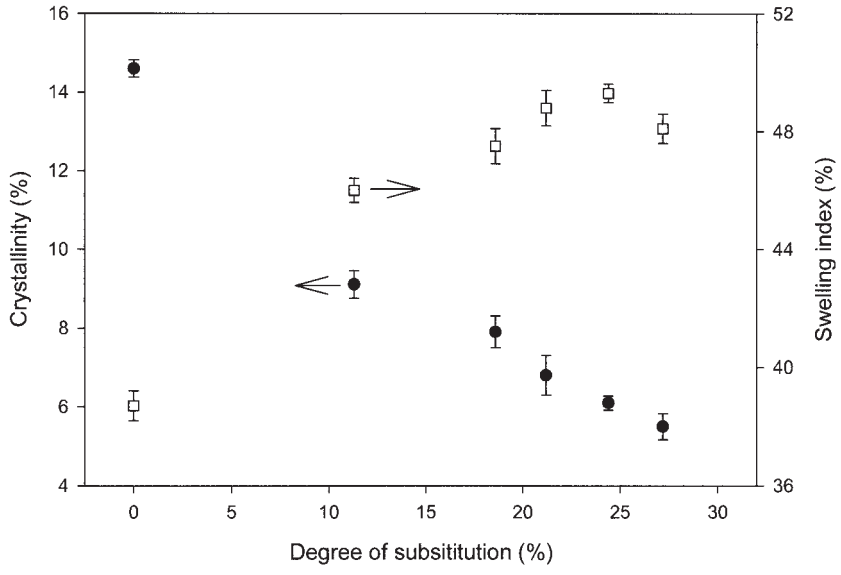

Figure 10 Crystallinity and swelling index of chitosan and di-*o*-butyrylchitosan membranes (ChT set).

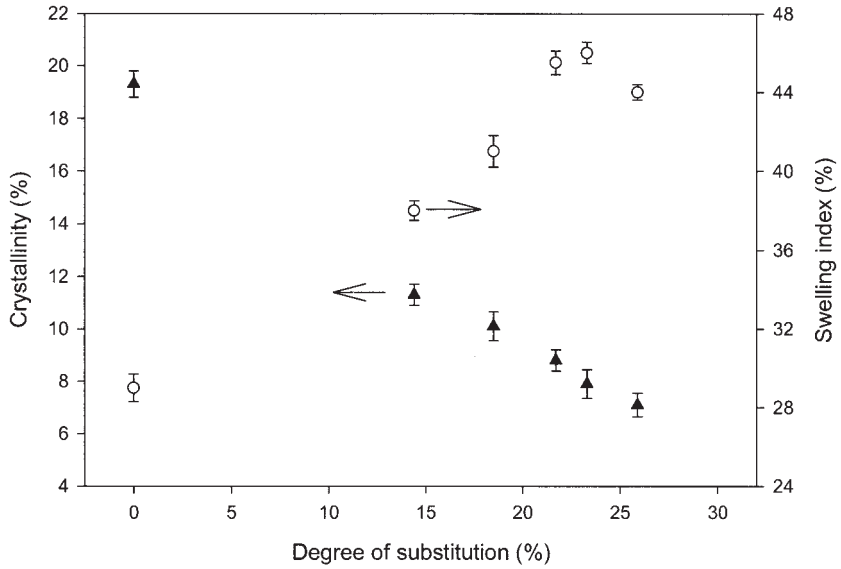

Figure 11 Crystallinity and swelling index of chitosan and di-*o*-butyrylchitosan membranes (ChT2 set).

brane prevents water from entering the membrane so that, the larger the crystallinity of a chitosan membrane is, the smaller the swelling index of the membrane.[38] As expected, after some bulky butyryl groups are incorporated into chitosan, the crystallinity of modified membranes is decreased, and corresponding swelling indices are increased. However, it is readily seen that the butyryl group has a dual character resulting from its polar carbonyl group (hydrophilic groups) and its nonpolar methylenic chain (hydrophobic chain). When the degree of substitution is increased, the percent content of methylenic side chains in di-*o*-butyrylchitosan will also be increased. Although the crystallinity of the membrane is decreased when the degree of substitution is higher (which helps to increase the swelling index of the membrane), the hydrophilicity of the membrane will also be decreased because of a higher content of methylenic side chains, which certainly decreases the swelling index of the membrane. Consequently, the swelling index of membranes decreases instead of increasing after a critical degree of substitution value is reached.

In addition, it was also found that the time for the swelling equilibrium of the modified membrane varied with the degree of substitution at a different rate. However, one hour is quite enough for all modified membranes to reach their swelling equilibrium. Since this issue is not a very important factor for the property of the modified membrane, and in most cases the modified membranes will work under a fully hydrated state in the application of fuel cell, the details for the swelling dynamics of the modified membrane in water have not been investigated further.

Thermal properties

Figure 12 exhibits the thermogravimetric analyses of chitosan and di-*o*-butyrylchitosan membranes. The onset temperature of thermal degradation of ChT takes place at a maximum rate at about 263°C, and the corresponding value for ChT2 is shifted to around 277°C. In general, it is known that hydrogen bonds between polymer chains contribute to raising the degradation temperature. As shown previously in Table I, ChT2 has a higher DDA, which will facilitate the intermolecular and intramolecular hydrogen-bond formation,[39] and thus, ChT2 should show a little higher degradation temperature than that of ChT.

The dependence of the onset temperature of thermal degradation on the degree of substitution, for di-*o*-butyrylchitosan membranes, is shown in Figure 13. It can be observed that the onset temperature of degradation increases gradually with degree of substitution, and is shifted significantly to a higher temperature when the degree of substitution is higher than 20%. Since intermolecular and intramolecular hydrogen-bonding play an important role in the crystalline structure of modified membranes, and affect their onset temperatures of degradation, the modified membrane with a higher degree of substitution should show a little lower onset temperature of degradation compared with unmodified membranes because of the lower crystallinity of modified membranes. However, the alteration of onset temperature of degradation in Figure 13 shows an opposite trend for all modified membranes. This observation may be attributed to the characteristic structure of di-*o*-butyrylchitosan membranes. From the structure described in Figure

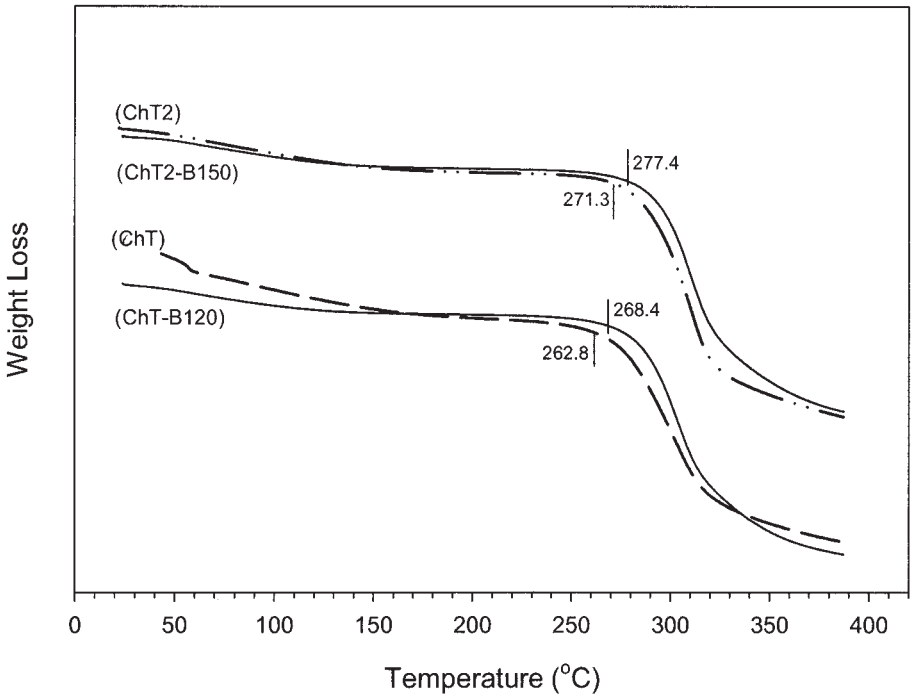

Figure 12 TGA thermograms of chitosan and di-*o*-butyrylchitosan membranes.

6, some hydroxyl groups are replaced by longer and bulkier butyryl groups, which results in a loss of hydrogen bonding in the membranes and may decrease its thermal degradation temperature if only one factor, hydrogen bonding, has been taken into account. But these longer and bulkier butyryl groups, on the other hand, can also be much more easily hooked to each other than the original hydroxyl groups at C-6 position, and perhaps lead to some extent of interlocking between them, and thus render a modified membrane with a higher onset temperature of degradation. The behavior of the onset temperature of degradation in Figure 13 may suggest that the effect from hooked chains in modified membranes is much stronger than that from hydrogen bonding and, as a result, the di-*o*-butyrylchitosan membrane with a relatively high degree of substitution exhibits an increased onset temperature of thermal degradation.

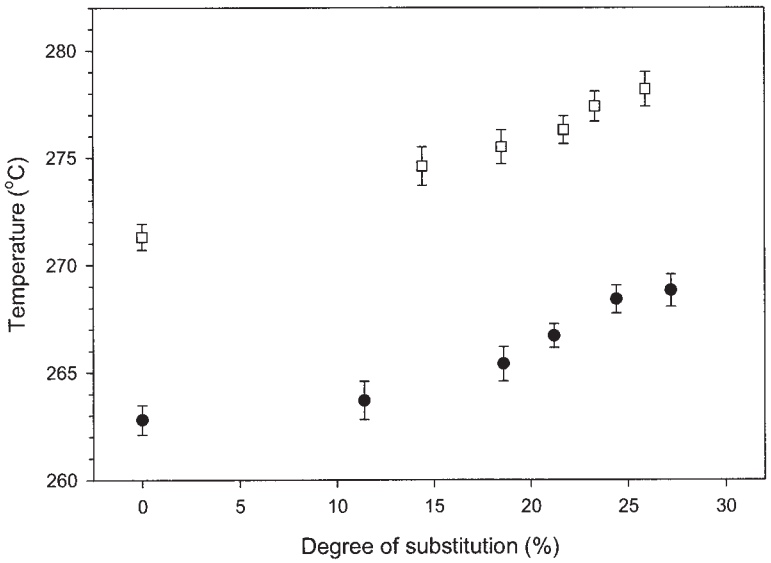

Figure 13 Dependence of onset temperature of thermal degradation on the degree of substitution for chitosan and di-*o*-butyrylchitosan membranes: □ - ChT2 set; ● - ChT set.

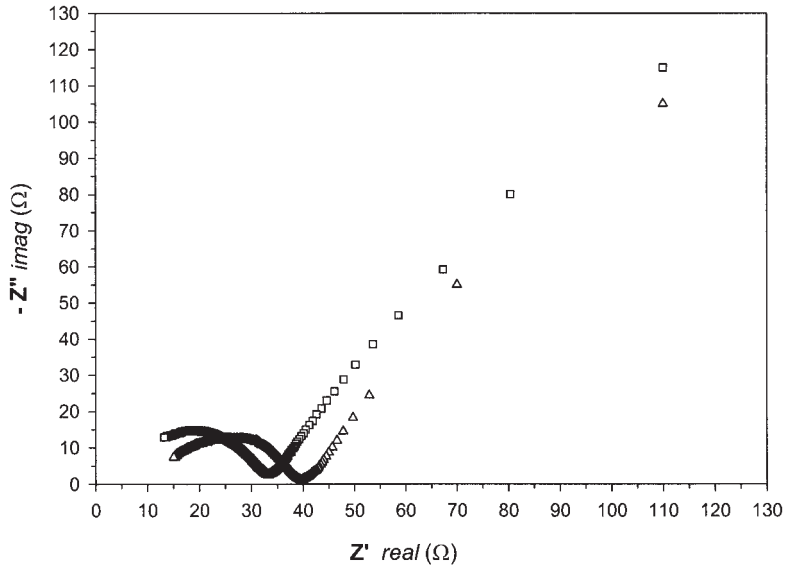

Figure 14 Impedance spectra of chitosan membranes after hydration for 1 h at 25°C: Δ - ChT2; □ - ChT.

Ionic conductivity of di-*o*-butyrylchitosan chitosan membranes

The ionic conductivity, of the di-*o*-butyrylchitosan membranes, was determined using complex impedance. Typical complex-plane plots of imaginary impedance (-Z'') versus real impedance (Z') for the membranes, after hydration for 1 h at room temperature, are illustrated in Figures 14 and 15. These spectra comprise two regions in the complex-plane, a partial semicircle arc in the high frequency zone that is related to the conduction process in the bulk of the membrane, and a linear region in the low frequency zone, being related to the existence of concentration gradients that give rise to diffusion processes in the bulk electrolyte.[40] They are likely to be similar to the impedance spectrum for Nafion® 117.[41] Since the complex impedance will be dominated by the ionic conductance, when the phase angle is close to zero, normally, the bulk resistance can be directly obtained from the intercept of the complex impedance plot with the real axis (Z' axis). If complex impedance curves have not touched the real axis, though they are near to the real axis, the impedance plot is extrapolated to its intersection with the real axis, and then the ionic con-

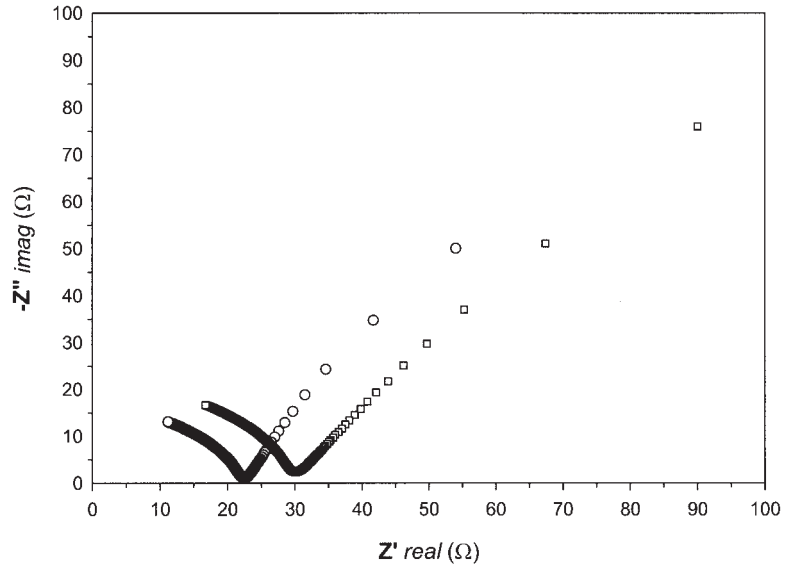

Figure 15 Impedance spectra of di-*o*-butyrylchitosan membranes after hydration for 1 h at 25°C: ○ - ChT-B120; □ - ChT2-B150.

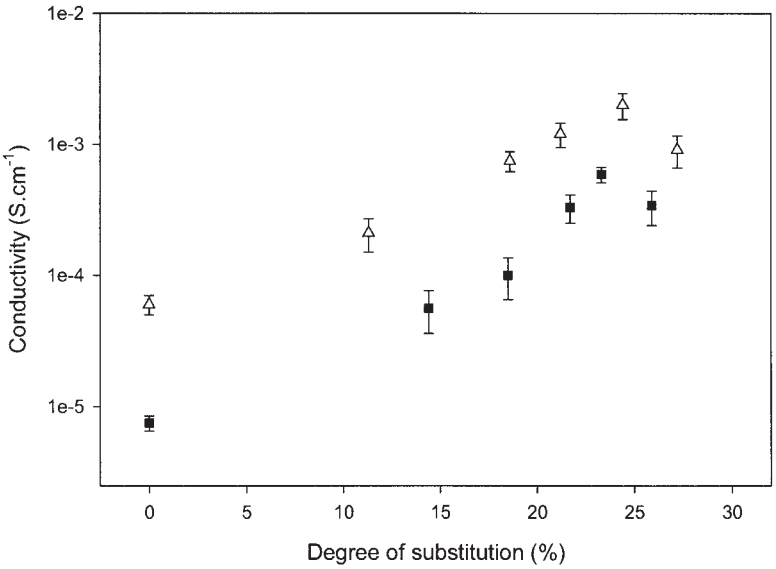

Figure 16 Ionic conductivity of di-*o*-butyrylchitosan membranes after hydration for 1 h at 25°C: Δ - ChT set; ■ - ChT2 set.

ductivity of the membrane is calculated using the Osman's method.[42]

All impedance measurements were done before and after hydration of the membranes. All membranes in the dry state exhibit ionic conductivities between 10^{-10} and 10^{-11} S cm^{-1} and the entire conduction process only occurs after the water is incorporated in the membranes. The variances in the conductivities of di-*o*-butyrylchitosan membranes, after hydration, are represented in Figure 16. The ionic conductivities of ChT-B120 and ChT2-B150 show a significant increase, compared with the corresponding unmodified membranes, by more than one order of magnitude. In particular, the ionic conductivity of ChT-B120 is also higher than that of those membranes that have been reported in our previous work.[16,17] From the fact that the ionic conductance occurs only after the membrane is hydrated, it can be concluded that the hydrated pattern of membranes will critically affect the ionic permeability through the membrane, such that a membrane with a relatively high swelling index may allow ions to pass through more easily in the swollen state of the membrane. Figures 10 and 11 indicate that the swelling indices of some modified membranes (for example, ChT-B90, ChT-B120, ChT2-B120, and ChT2-B150) are higher than unmodified membranes and, as expected, their corresponding conductivities in Figure 16 are also higher. Accordingly, ChT-B150 and ChT2-B180 show relatively low conductivities due to their lower swelling indices seen by comparing Figure 16 with Figure 10 or Figure 11. According to a possible mechanism described in our previous work[15] for ionic conductivity, a higher -NH_2 content in chitosan membranes is expected to contribute to a higher ionic conductivity. However, it is observed that each sample in the ChT set (lower -NH_2 content and lower DDA value) shows a slightly higher conductivity than the corresponding one in the ChT2 set (higher -NH_2 content and higher DDA value). This may be understood by looking at the difference in crystalline properties between the two sets of samples. As shown in Figures 10 and 11, each sample in the ChT2 set has a higher crystallinity than that in the ChT set with a similar degree of substitution. This means, for each sample in the ChT2 set, more crystalline regions should be formed because of its higher DDA,[36] and as a consequence, water is prevented from entering the crystalline portion leading to a smaller water incorporation into the membrane. This consequently decreases the concentration of OH^- groups in the swollen membrane and in turn the ionic conductivity of modified membranes. The above results may suggest that the -NH_2 content is not the most important factor for the ionic conductivity in these modified membranes and that the DDA value of modified membranes should not be kept too high.

As a hydroxide ion conductor, the di-*o*-butyrylchitosan membrane may be useful for an alkaline polyelectrolyte fuel cell (PEFC) where a carrier type of membrane for hydroxide ion transport is needed. Among various polyelectrolyte membranes used for PEFC, the perfluorinated membranes have been considered as the most effective and available membranes that are used in practical systems.[43] One of the perfluorinated membranes, Nafion® N117, has an ionic conductivity in its swollen state of around 2.6×10^{-2} $S.cm^{-1}$ and has a relatively long lifetime.[44,45] In spite of their superior characteristics for PEFCs, these membranes do have some weak points.[46] They are strongly limited to the range of temperature within which they

can be reliably used. The upper operation temperature limit is usually considered to be 100°C because of their low water content above that temperature (and hence lower ionic conductivity), and because of accelerated oxidative degradation. In addition, their relatively high cost may also limit their use in mass production of fuel cells. Although the ionic conductivity of the di-*o*-butyrylchitosan membranes (ChT-B120 and ChT2-B150) is not as high as that of the Nafion® N117 membrane, these membranes exhibit swelling indices of more than 45% and conductivities of $\sim 10^{-3}$ S.cm^{-1}, which are adequate for fuel-cell operation.[47] In particular, a fundamental difference in the ionic functionality between the Nafion® membrane and di-*o*-butyrylchitosan membranes has to be pointed out, that is, the Nafion® membrane is a proton conductor and it only can be used for an acidic polymer electrolyte fuel cell,[48] while the di-*o*-butyrylchitosan membrane may be used for an alkaline polymer electrolyte fuel cell as a hydroxide ion conductor. Further results for applications in PEFC will be given in a separate report.

CONCLUSION

Di-*o*-butyrylchitosan was prepared by reacting chitosan with butyric acid anhydride in the presence of perchloric acid as a catalyst. The results from IR and ^{13}C-NMR spectra suggest that both hydroxyl groups at the C-6 and the C-3 positions in chitosan units were substituted. The degree of substitution, obtained by integrating ^{1}H-NMR spectra of unmodified and modified chitosan, yielded a maximum degree of substitution of 28% under present reaction conditions. Some properties of the modified membranes have been remarkably changed from those of unmodified chitosan membranes. The crystallinity of modified membranes decreases with increasing degree of substitution and, at the same time, their swelling indices (SI) increase to a maximum value and then drop off slightly. Some modified membranes with a higher degree of substitution unexpectedly show an increase in thermal stability as derived from their onset temperature of thermal degradation. The ionic conductivity, of modified chitosan membranes after hydration, has been significantly improved compared to unmodified chitosan membranes, and some of them, with an appropriate degree of substitution, show an increase in the ionic conductivity of more than one order of magnitude.

The financial support for this work was provided by the National Science and Engineering Council of Canada under grant NO. 239090–01. Thanks are due to Dr. F. Sauriol from Queen's University for her valuable assistance in NMR measurements.

References

1. Hudson, M. S. In Adv in Chitin Science, Vol. II, Proceedings of the 7th International Conference on Chitin and Chitosan, Lyon, France, 1997; Domard, A.; Varum, K.; Muzzarelli, R., Eds.; Jaques Andre publisher: Lyon, 1998; p. 590.
2. Mcgahren, W. J.; Perkinson, G. A.; Growich, J. A.; Leese, R. A.; Ellestad, G. A. Process Biochem 1984, 19, 88.
3. Shahidi, F. Canadian Chem News 1995, 47, 25.
4. Kurita, K. In Functional Polymers, Synthesis and Application; Arshady, R., Ed.; American Chem Society: Washington, 1996; p. 240.
5. Rathke, T.; Hudson, S. J Macromol Sci Rev Macromol Chem Phys 1994, C34, 375.
6. Krajewska, B. J Chem Technol Biotechnol 2001, 76, 636.
7. Uragami, T.; Yoshida, F.; Sugihara, M. Makromol Chem Rapid Commun 1983, 4, 99.
8. Nishimura, S. I.; Kohgo, O.; Kurita, K.; Kuzuhara, H. Macromolecules 1991, 24, 4745.
9. Uragami, T.; Matsuda, T.; Okuno H.; Miyata, T. J Membr Sci 1994, 88, 243.
10. Nishi, N.; Noguchi, J.; Tokura S.; Shiota, H. Polym J 1979, 11, 27.
11. Tokura, S.; Nishi, N.; Somorin, O.; Noguchi, J. Polym J 1980, 12, 695.
12. Nishi, N.; Ohnuma, H.; Nishimura, S.; Somorin, O.; Tokura, S. Polym J 1982, 14, 919.
13. Somorin, O.; Nishi, N.; Tokura, S.; Noguchi, J. Polym J 1979, 11, 391.
14. Kaifu, K.; Nishi, N.; Komai, T.; Tokura, S.; Somorin, O. Polym J 1981, 13, 241.
15. Wan, Y.; Creber, K. A. M.; Peppley, B.; Bui, V. T. Polymer 2003, 44, 1057.
16. Wan, Y.; Creber, K. A. M.; Peppley, B.; Bui, V. T. J Appl Polym Sci 2003, 89, 306.
17. Wan, Y.; Creber, K. A. M.; Peppley, B.; Bui, V. T. Macromol Chem Phys 2003, 204, 850.
18. Muzzarelli, R. A. A.; Jeuniaux, C.; Gooday, G. W. Chitin in Nature and Technology; Plenum: New York, 1986; p. 385.
19. Knaul, J. Z.; Kasaai, M. R.; Bui, V. T.; Creber, K. A. M. Can J Chem 1998, 76, 1699.
20. Kasaai, M. R.; Charlet G.; Arul, J. In Adv in Chitin Science, Vol. II, Proceedings of the 7th International Conference on Chitin and Chitosan; Domard, A.; Roberts, G. A. F.; Varum, K., Eds.; Jaques Andre: Lyon, France, 1997; Vol. 2, p. 421.
21. Szosland, L.; East, G. C. J Appl Polym Sci 1995, 58, 2459.
22. Hiral, A.; Odanl, H.; Nakajima, A. Polym Bull 1991, 26, 87.
23. Rabek, J. K. Experimental Methods in Polymer Chemistry: Applications of Wide-Angle X-Ray Diffraction (WAXD) to the Study of the Structure of Polymers; Wiley-Inter Science: Chichester, UK, 1980; p. 505.
24. Mokrini, A.; Acosta, L. J. Polymer 2001, 42, 8817.
25. Roberts, G. A. F. Chitin Chemistry; Macmillian Press Ltd.: London, 1992; p. 65.
26. Mima, S.; Miya, M.; Iwamoto, R.; Yoshikawa, S. J Appl Polym Sci 1983, 28, 1909.
27. Tual, C.; Espuche, C. T.; Escobes, M.; Domard, A. J Polym Sci Part B: Polym Phys 2000, 38, 1521.
28. Li, Z.; Zhuang, X. P.; Liu, X. F.; Guan, Y. L.; Yao, K. D. Polymer 2002, 43, 1541.
29. Xie, W.; Xu, P.; Wang, W.; Liu, Q. Carbohydr Polym 2002, 50, 35.
30. Heras, A.; Rodriguez, N. M.; Ramo, V. M.; Agollo, E. Carbohydr Polym 2001, 44, 1.
31. Varum, K. M.; Anthonsen, M. W.; Grasdalen, H.; Smidserod, O. Carbohydr Res 1991, 217, 19.
32. Saito, H.; Tabuta, R.; Hirano, S. In Proceedings of the First Symposium on Chitin and Chitosan, Osaka, Japan, August 1981; p. 31.
33. Usui, T.; Ysmsnsks, N.; Matsuda, K.; Tsujimura, K.; Sugiyama, H.; Seto, H. J Chem Soc Perkin Trans 1973, 1, 2425.
34. Tokura, S.; Yoshida, J.; Nishi, N.; Hiraoki, T. Polym J 1982, 14, 527.

35. Cha, S. Y.; Lee, J. K.; Lim, B. S.; Lee, T. S.; Park, W. H. J Polym Sci Part A: Polym Chem 2001, 39, 880.
36. Chen, R. H.; Lin, J. H.; Yang, M. H. Carbohydr Polym 1996, 31, 141.
37. Samuels, R. J. J. J Polym Sci Polym Phys Ed 1981, 19, 1081.
38. Chen, R. H.; Hwa, H.-D. In Adv in Chitin Science, Volume I; Domard, A.; Jeuniaux, C.; Muzzarelli, R.; Roberts, G., Eds.; Jacque Andre Publisher: Lyon, France, 1996; p. 346.
39. Anthonsen, W. M.; Varum, K. M.; Smidsrod, O. Carbohydr Polym 1993, 22, 193.
40. Beattie, P. D.; Orfino, F. P.;; Basura, V. I.; Zychowska, K.; Ding, J.; Chuy, C.; Schmeisser, J.; Holdcroft, S. J Electroanal Chem 2001, 503, 45.
41. Gardner, C. L.; Anantaraman, A. V. J Electroanal Chem 1995, 395, 67.
42. Osman, Z.; Ibrahim, Z. A.; Arof, A. K. Carbohydr Polym 2001, 44, 167.
43. Gottesfeld, S.; Zawodzinski, T. A. Adv Electrochem Sci Eng 1997, 5, 195.
44. Sumner, J. J.; Creager, S. E.; Ma, J. J.; DesMarteau, D. D. J Electrochem Soc 1998, 145, 107.
45. Sondheimer, S. J.; Bunce, N. J.; Fyfe, C. A. J Macromol Sci Rev Macromol Chem Phys 1986, C26, 353.
46. Savadogo, O. J. New Mat Electrochem Systems 1998, 1, 47.
47. Zawodzinski, T. A.; Derouin, J. C.; Radzinski, S.; Sherman, R. J.; Smith, V. T.; Springer, T. E.; Gottesfeld, S. J Electrochem Soc 1993, 140, 1041.
48. Blomen, L. J. M. J.; Mugerwa, M. N. Fuel Cell System; Plenum Press: New York, 1993.